146

RESPONSE OF GUARDRAIL POSTS DURING IMPACT

by
Jarvis D. Michie

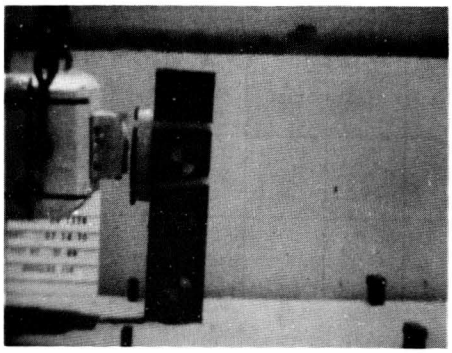

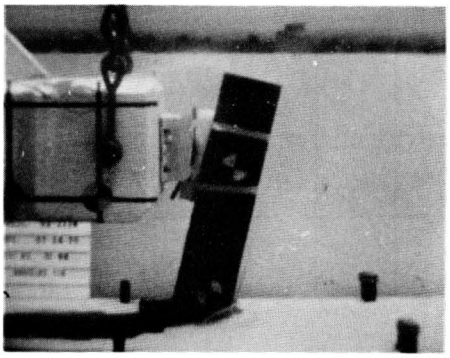

FINAL REPORT
IR Project No. 03-9051

Prepared for

Technical Planning Council
Southwest Research Institute

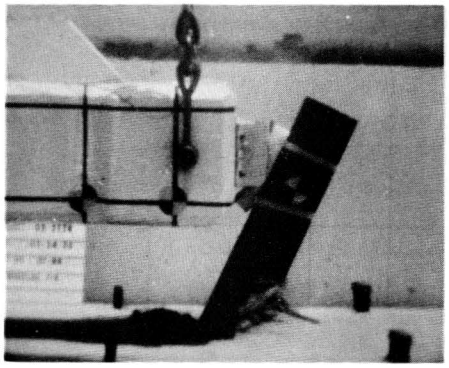

October 15, 1970

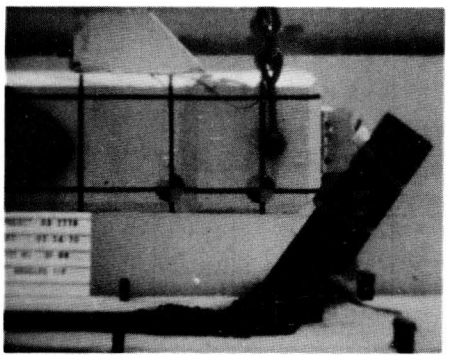

SOUTHWEST RESEARCH INSTITUTE
SAN ANTONIO HOUSTON

SOUTHWEST RESEARCH INSTITUTE
Post Office Drawer 28510, 8500 Culebra Road
San Antonio, Texas 78228

RESPONSE OF GUARDRAIL POSTS DURING IMPACT

by
Jarvis D. Michie

Final Report
IR Project No. 03-9051

Prepared for
Technical Planning Council
Southwest Research Institute

October 15, 1970

Approved:

Robert C. DeHart

Robert C. DeHart, Director
Department of Structural Research

ABSTRACT

An experimental program was performed to acquire data that characterize the response of partially embedded posts during impact. Two types of noncohesive soils, three specimen widths, and four specimen embedment depths were examined. Specimens were impacted by a 4000-lb mass traveling at velocities of 15, 20, and 30 fps. The experimental information obtained consists of linear impulse, peak and average resistance forces, and kinetic energy absorbed by the post/soil system.

Findings indicate that post/soil system dynamic response varies with soil strength, specimen width, and embedment depth. Dynamic responses are from 2 to 4 times the corresponding static response for the post/soil system.

TABLE OF CONTENTS

	Page
LIST OF ILLUSTRATIONS	*vi*
LIST OF TABLES	*vi*
I. INTRODUCTION	1
II. EXPERIMENTATION PROCEDURE	2
A. Test Apparatus	2
B. Soils	4
C. Specimens	5
D. Test Procedure	5
E. Program Scope	6
III. FINDINGS	7
IV. DISCUSSION	13
A. Experimental Procedure	13
B. Post/Soil Parameters	14
V. CONCLUSIONS	15
A. Soil Effects	15
B. Embedment Geometry	15
C. Relationship of Static-to-Dynamic Results	15
APPENDIX A—SAMPLE CALCULATIONS	A-1
APPENDIX B—SAMPLE IMPULSE PLOTS	B-1

LIST OF ILLUSTRATIONS

Figure		Page
1	Typical guardrail installation after vehicle impact.	1
2	SwRI pendulum impact tester.	2
3	Post/soil test design features.	2
4	Typical experiment features prior to test.	3
5	Apparatus for determining static force-deflection properties of post/soil system.	3
6	Standard penetration.	4
7	Approximate allowable soil pressure for footings as a function of penetration resistance.	4
8	Gradation of test soils.	5
9	Typical post resistance versus time plot.	7
10	Relationship of post/soil system impulse with embedment.	10
11	Relationship of post/soil system kinetic energy dissipation with post embedment.	10
12	Relationship of post/soil average resistance force with post embedment.	11
13	Comparison of static and dynamic force deflection curves for Soil Type 1.	11
14	Comparison of static and dynamic force deflection curves for Soil Type 2.	11
15	Typical post/soil failure characteristics.	12

LIST OF TABLES

Table		Page
1	Test conditions.	6
2	Summary of results: Soil Type 1.	8
3	Summary of results: Soil Type 2.	9
4	Comparison of dynamic and static post/soil test results.	12

I. INTRODUCTION

In typical highway guardrail installations as shown in Figure 1, the posts are subjected to dynamically applied horizontal forces. Under this loading, the posts may (1) deform elastically, (2) fracture, or (3) be pushed over due to failure in the embedment soil; frequently, a post exhibits a combination of these three behavioral characteristics. Accordingly, performance of posts reflects both post properties (i.e., material strength, post geometry, etc.) and soil properties (i.e., shear strength, density, etc.).

Figure 1. Typical guardrail installation after vehicle impact.

A guardrail system dynamic performance is evaluated in terms of vehicle redirection accelerations and rebound trajectory. Theoretical analyses of the guardrail-vehicle interaction reveal that these performance criteria (i.e., vehicle accelerations and trajectory) are significantly influenced by the post/soil behavior. Heretofore, little experimental work has been performed in this particular area of soil dynamics; hence, it has been necessary to estimate post/soil behavior for use in theoretical guardrail performance computations.

This report describes the preliminary effort by Southwest Research Institute to investigate the basic behavior of post/soil interaction. The objective of the program was to experimentally study the behavior of posts partially embedded in soil during impact with a heavy mass. The test facilities and experimentation procedures are described in Section II, and the summary of tests and results is presented in Section III. In Section IV, program results are discussed; conclusions are presented in Section V.

II. EXPERIMENTATION PROCEDURE

The test apparatus and procedures are designed to subject specimens to the type of loading experienced by highway guardrail posts when the guardrail system is impacted by an errant vehicle.

A. Test Apparatus

1. Pendulum

The pendulum impact facility consists of pendulum, operating equipment, and test control and data acquisition instrumentation. An overall view of the facility is shown in Figure 2. A 4000-lb mass is suspended in such a manner that it remains horizontal throughout the normal swing arc of 26-ft radius. Other weights and mass geometries may be used; however, the 4000-lb mass was selected for this program because it represents the weight of a medium size passenger car.

Impact velocity is controlled by adjusting the vertical fall of the mass and is calculated by the expression

$$V_I = \sqrt{2gh}$$

where V_I is impact velocity (ft/sec), g is acceleration due to gravity (32.2 ft/sec^2), and h is the mass drop height (ft). Impact velocities ranging from 0 to 40 fps are obtainable within the available 25-ft drop height.

Test specimens are stationed at the lowest point of the pendulum arc where the kinetic energy (i.e., velocity) of the mass is maximum. The pendulum mass strikes the embedded posts at a point 24 in. above grade, as shown in Figure 3, and remains in contact

Figure 2. SwRI pendulum impact tester.

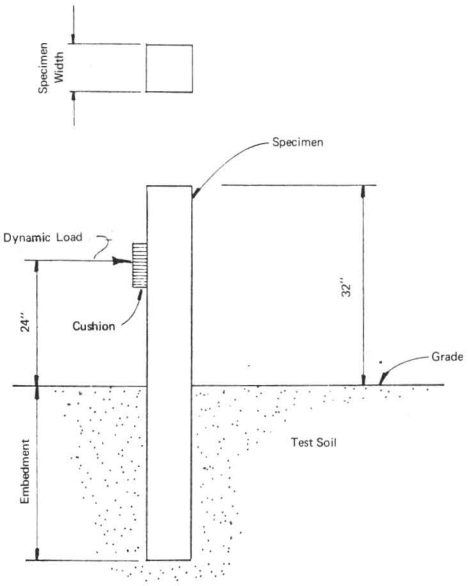

Figure 3. Post/soil test design features.

with the specimen until the post is pushed over and down underneath the mass. A view of the experiment features is shown in Figure 4. It should be noted that the mass rises about 4 in. during post contact (about 4-ft horizontal displacement) due to the swing arc, and results in an increase (i.e., 4 in.) in the overturning moment arm.

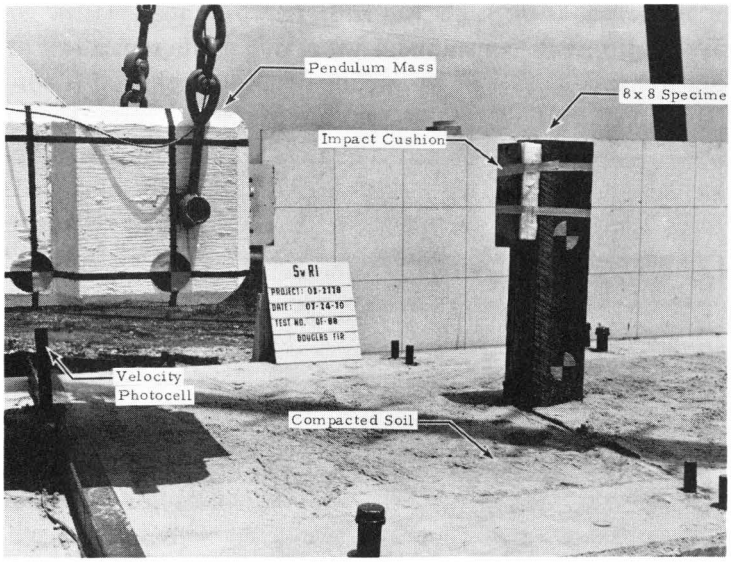

Figure 4. Typical experiment features prior to test.

Instrumentation consists of a velocity sensor and accelerometers. A photocell located immediately upstream from the specimen triggers on light reflecting strips attached to the lower surface of the pendulum mass. As the pendulum mass moves past the photocell, the device is triggered by the incrementally spaced strips and produces signal pulses. An accelerometer*, rigidly mounted to the pendulum mass, senses the mass horizontal deceleration magnitudes caused by the specimen/soil resisting force. Accordingly, the post resisting force is determined continuously throughout impact by multiplying mass deceleration by mass weight. Signals from the velocity photocells and accelerometer are recorded on magnetic tape. A visual record (strip-chart) of the raw data is also produced during a test to provide preliminary information and to insure that instrumentation systems are functioning properly.

2. *Static Test Lorry*

A special lorry is used to acquire the static force-deflection characteristic of the post/soil system. As shown in Figure 5, the apparatus is pulled against and over the

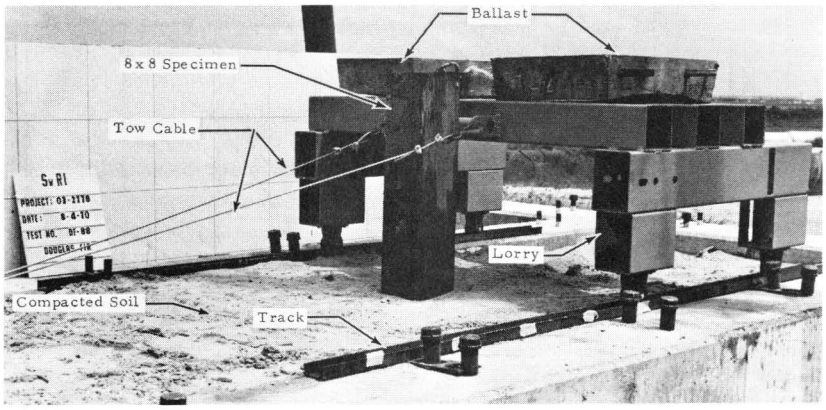

Figure 5. Apparatus for determining static force-deflection properties of post/soil system.

*Linear strain gage accelerometer, CEC Type No. 4-202-0001, ±25-g range.

specimen as it deforms the soil. The principal feature of the device is that the point of load application is a constant 24 in. above grade regardless of post displacement. Post/soil resisting force is measured by means of a load cell that is connected in series with the tow cables (the load cell is not shown in Figure 5); the load cell output signal is continuously recorded during the test. Displacements are visually observed and manually superimposed on the load cell strip-chart trace.

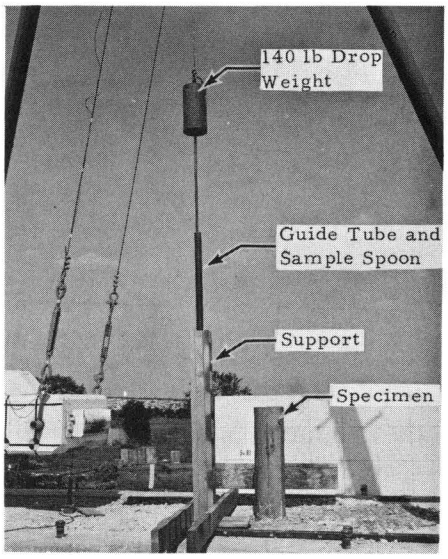

(a) Soil Test Apparatus

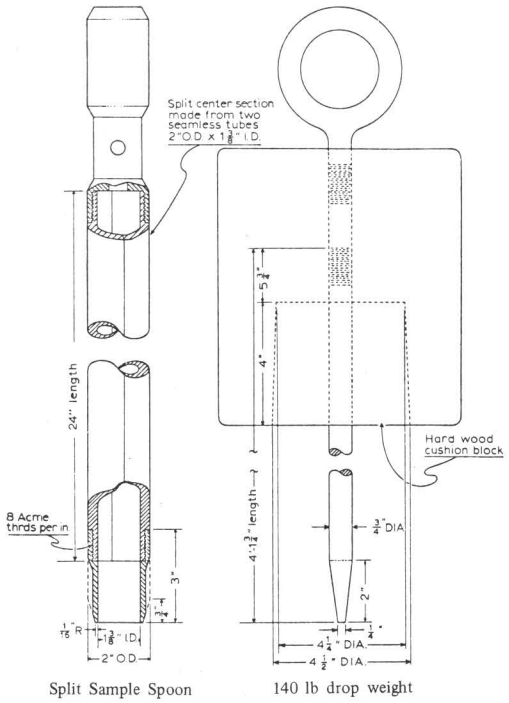

(b) Penetrometer Detail

Figure 6. Standard penetration test.

3. Penetrometer

To establish that the soil is compacted to a referenced density, a standard penetration test using a penetrometer is performed prior to an experiment. The penetrometer apparatus is shown in Figure 6. The principle of operation is based on the number of blows (i.e., 140-lb weight dropped from a 30-in. height) required to drive the sample spoon 12 in. into the soil. Penetrometer test results can be empirically related to soil density and bearing strength. Some typical values for various soils are depicted in Figure 7.

B. Soils

Noncohesive soils were selected for the program in lieu of cohesive materials because they are more readily compacted to a reference

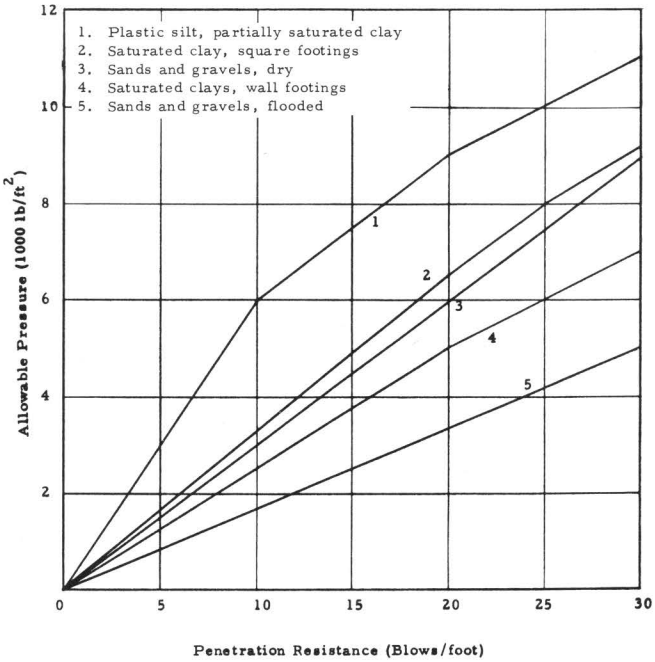

Figure 7. Approximate allowable soil pressure for footings as a function of penetration resistance.

density prior to a test. Also, the strength of noncohesive soils is less affected by moisture content; the noncohesive soils exhibit a minimum thixotropical characteristic. Hence, soil test controls are less critical.

To provide a range of soil strength, a uniformly graded sand and a well-graded gravel were selected. Typical gradation plots and densities for the two soils are shown in Figure 8. The sand, referred to as Soil Type 1, is common material used in production of concrete; the gravel, referred to as Soil Type 2, is a special highway base material specified by the Texas Highway Department.

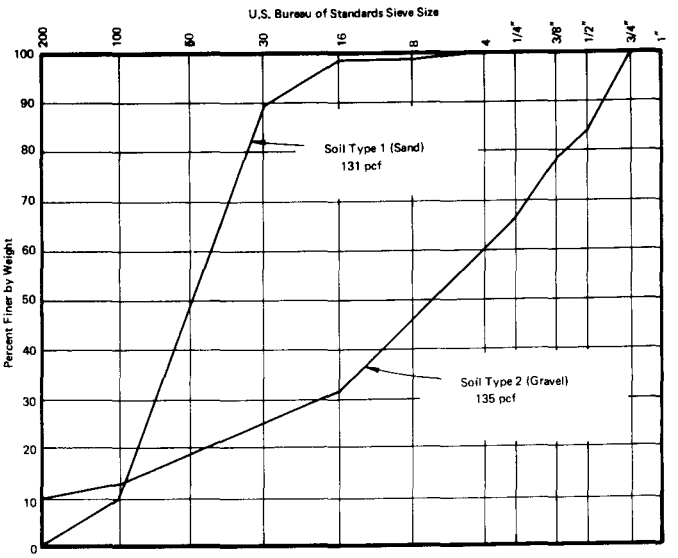

Figure 8. Gradation of test soils.

C. Specimens

Post specimens were typical timber shapes used in highway traffic barrier construction. The wood species used was, in general, Douglas fir; however, red oak was used in several tests where increased material strength was desired.

Principal specimen dimensions were post width and embedment length. Length of post above grade was maintained at a consistent 32 inches; hence, for the shallow embedment tests, the post specimens were reduced in overall length. Embedment length was varied from 20 to 40 inches.

As the objective of the program was to investigate soil properties, post specimen size was selected so that the post would not fracture or otherwise fail during the dynamic loading. Even so, post strength was exceeded prior to soil failure in several cases.

D. Test Procedure

Geometry of post specimens was measured, and the linear dimensions were recorded. A SwRI test number was assigned to specimen.

For the Soil Type I (sand) tests, the specimen was located in the test bed and held temporarily in the desired position by timber struts. Sand was flooded with water around the post to achieve a consistent soil density; the timber struts were removed, and water was allowed to drain from the bed for a period of 10 min immediately prior to the test.

For the Soil Type 2 (gravel), the disturbed material from the previous test was removed and then replaced in 6-in. layers; each layer was densified by a pneumatic compacter. Water was periodically added to the test bed to promote soil consolidation; however, no attempt was made to control the moisture content of the soil.

A standard penetrometer test of the prepared test bed was conducted immediately prior to a limited number of tests. Results of these tests were fairly consistent with Soil Type 1 exhibiting 0.6 blow per foot resistance; Soil Type 2 resistance ranged from 10 to 13 blows per foot.

1. Static Test

The lorry was positioned against the test specimen as shown in Figure 5; the instrumentation system was energized and a calibrated signal transmitted via the circuit and recorded on the strip-chart. On signal from the test engineer, the lorry was pulled against and over the specimen at a slow and near constant rate. As the lorry passed calibrated points, the strip-chart was manually marked. The test was terminated when the lorry and specimen had been displaced 4 ft.

Table 1. Test conditions.

Post Embedment Depth h (in.)	Number of Tests Post Width b (in.)		
	4	6	8
10	3	3	3
20	3	3	3
30	3	3	3
40	3	3	3
Total Tests for Soil Type			36
		Tests	
Soil Type 1		36	
Soil Type 2		36	
Total Tests		72	

2. Dynamic Test

Mechanics of the test were simple. Instrumentation systems were first energized and calibrated. The mass was pulled away from the impact point until its elevation provided the preselected drop height. On signal from the test engineer, the pendulum mass was released by means of a quick-release mechanism. Instrumentation signals were recorded from mass release through impact and swing-through. Duration of impact varied from 68* to 510 ms.

E. Program Scope

As shown in Table I, the basic program consisted of 72 experimental tests. Two soil types, four embedment depths, and three post widths were planned. Midway in the program, the scope was slightly modified by substituting 35-in. embedment depth tests for the planned 10-in. depth tests.

*Excludes tests in which post failed..

III. FINDINGS

Findings from the program are in the form of experimental data that define the gross behavior of partially embedded post specimens that are subjected to a dynamically applied horizontal displacement. Primary data are plots of specimen resistance force as a function of time for each test case; a typical plot is illustrated in Figure 9 for an 8-in.-wide post embedded 30 in. in Soil Type 2. From this basic plot, the total impulse imparted to the pendulum mass is determined by integrating the area under the curve. Work performed on the post/soil system is the change in the kinetic energy of the pendulum mass. An average post/soil resistance force F is determined by dividing work or change in kinetic energy by the specimen displacement. Sample calculations used in the data reduction process are illustrated in Appendix A.

Two characteristic features of a typical impulse curve (see Fig. 9) are (1) the post inertia peak and (2) the soil shearing resistance. The inertia peak occurred between 5 and 15 ms after impact for the tests performed in this program. Magnitude of this initial peak appeared to be a direct function of impact velocity and post specimen mass. (A second inertia peak, exhibited in tests where embedment was 20 in., could be attributed to the momentum imparted to the soil.) The soil shearing phase of the plots is characterized by a rapid rise to a peak shearing force followed by a gradual decline. Representative curves for a majority of program tests are contained in Appendix B.

Test results are tabulated in Table 2 for Soil Type 1 and in Table 3 for Soil Type 2. Pretest soil condition and post embedment geometry are presented in the columns following specimen designation. Actual pendulum mass velocity at instant of impact is listed for each specimen; depending on the anticipated level of kinetic energy dissipation, target impact velocity was either 15, 20, or 30 fps. The most significant program results are considered to be linear impulse, impact duration, and kinetic energy dissipated (or work performed)

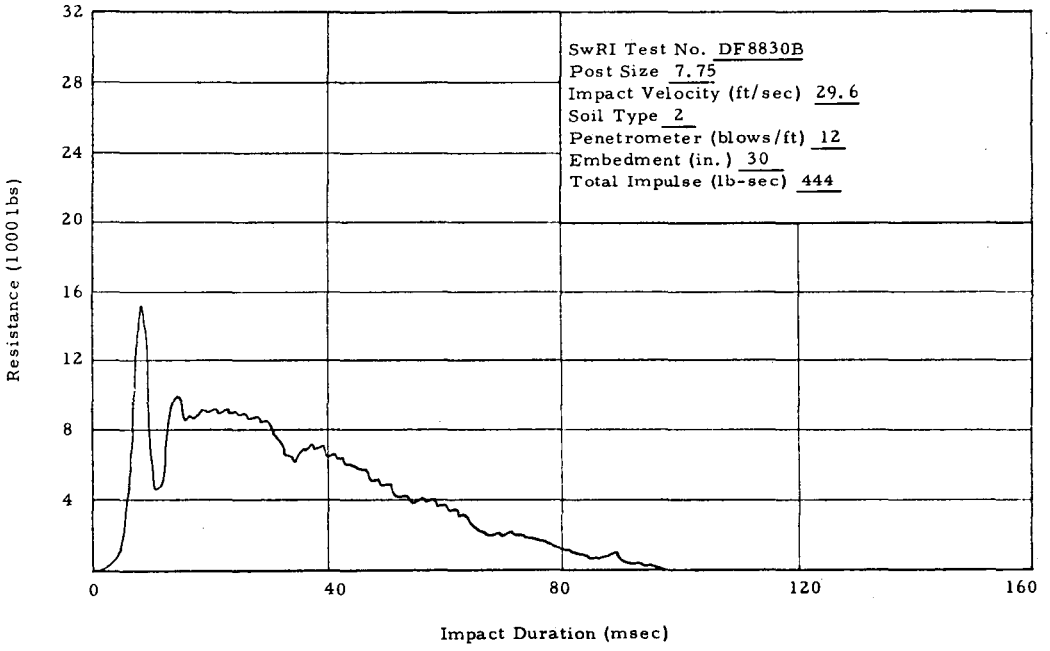

Figure 9. Typical post resistance versus time plot.

*Table 2. Summary of results: Soil Type 1.**

Specimen No.	Penetrometer (blows/ft)	Width (W, in.)	Embedment Depth (H, in.)	Impact Velocity (V_i, fps)	Impulse (MV, lb-sec)	Impact Duration (t, ms)	Kinetic Energy (KE, ft-kips)	Average Force (F, kips)
DF8840 A	0.7†	7.50	40	16.0	798	510	10.2	1.6
DF8840 B				15.5	862	500	10.3	1.7
DF8840 C				15.3	734	460	9.0	1.6
DF8840 D				14.8	862	470	9.7	1.8
DF8840 AA				14.7	711	459	8.4	1.6
Average				(15.26)	(793.4)	(479.8)	(9.52)	(1.66)
DF8830 A		7.50	30	15.1	606	440	7.70	1.4
DF8830 B				15.6	415	400	5.72	1.0
DF8830 C				15.2	596	390	7.63	1.5
DF8830 D				15.8	479	380	6.56	1.3
DF8830 AA				15.9	262	322	3.87	0.8
Average				(15.52)	(471.6)	(386.4)	(6.296)	(1.20)
DF8820 A		7.50	20	15.5	351	360	4.90	1.0
DF8820 B				15.9	319	320	4.72	1.0
DF8820 C				15.8	287	320	4.18	0.9
DF8820 D				17.5	255	310	4.10	0.8
DF8820 AA				15.3	163	301	2.36	0.5
Average				(16.0)	(275.0)	(322.2)	(4.052)	(0.84)
DF6640 A	0.7†	5.75	40	15.7	925	450	11.03	2.0
DF6640 B				15.2	643	379	8.14	1.7
DF6640 C				14.9	546	379	6.94	1.4
DF6640 D				15.1	437	356	5.80	1.2
Average				(15.22)	(637.8)	(391.0)	(7.978)	(1.58)
DF6630 A		5.75	30	15.3	248	329	3.55	0.8
DF6630 B				15.6	250	315	3.63	0.8
Average				(15.45)	(249)	(322)	(3.595)	(0.8)
DF6620 A		5.75	20	15.3	98	300	1.48	0.3
DF6620 B				15.4	100	296	1.49	0.3
Average				(15.35)	(99)	(298)	(1.485)	(0.3)
DF4440 A	0.7†	3.75	40	14.8	415	340	5.38	1.2
DF4440 B				16.3	479	360	6.80	1.3
DF4440 C				16.3	606	350	8.43	1.7
DF4440 D				15.1	447	320	5.95	1.4
DF4440 AA				15.9	331	376	4.88	0.9
Average				(15.68)	(455.6)	(349.2)	(6.288)	(1.30)
DF4430 A		3.75	30	15.2	134	314	2.00	0.4
DF4430 B				15.1	163	323	2.33	0.5
Average				(15.15)	(148.5)	(318.5)	(2.165)	(0.45)

*Sand with uniform gradation.
†One Blow = 18 inches.

by the post soil system. For use in highway guardrail theoretical predictions, an idealized or average force* (assumed constant throughout impact sequence) is shown.

Linear impulse or pendulum mass momentum change is plotted in Figure 10 against post embedment for the two soil types and three specimen widths. Soil Type 1 data are consistently lower than Soil Type 2 values. For both soils, impulse appears to be a direct function of both embedment depth and post width.

*See Appendix A for definition and determination.

*Table 3. Summary of results: Soil Type 2.**

Specimen No.	Penetrometer (blows/ft)	Width (W, in.)	Embedment Depth (H, in.)	Impact Velocity (V_i, fps)	Impulse (MV, lb-sec)	Impact Duration (t, ms)	Kinetic Energy (KE, ft-kips)	Average Force (F, kips)
DF8840 A	15	7.88	40	29.2	1545	221	35.4	7.0
DF8840 B	12	7.88	40	30.3	1344	154	33.4	8.7
Average				(29.75)	(1444.5)	(187.5)	(34.4)	(7.85)
DF8835		7.88	35	30.3	1220	210	30.9	6.1
DF8830 A	13	7.75	30	32.0	384	87	11.7	4.4
DF8830 B	12	7.75	30	29.6	444	99	12.4	4.5
Average				(30.8)	(414)	(93)	(12.05)	(4.45)
DF8820 A	10	7.75	20	30.3	213	76	6.2	2.8
DF8820 B	12	7.75	20	30.3	185	68	5.5	2.7
Average				(30.3)	(199)	(72)	(5.85)	(2.75)
DF6835		6.0	35	30.3	850	155	22.5	5.4
RO6430 A		6.12	30	19.5	623	168	10.6	3.7
RO6420 A		6.12	20	19.2	160	103	3.0	1.6
DF6620 A	12	6.0	20	30.3	143	79	4.4	1.8
DF6620 B	13	6.0	20	30.3	217	86	6.2	2.5
Average				(26.6)	(173.3)	(89.3)	(4.53)	(1.97)
DF4440 A†		4.0	40	30.3	32	32	0.8	1.0
DF4835		4.0	35	30.3	733	177	20.9	4.1
DF4430 A†		3.75	30	19.3	102	60	1.9	1.7
RO4630 A		4.0	30	19.1	507	152	8.7	3.3
DF4420 A		4.12	20	19.4	199	133	3.7	1.5

*Well-graded highway base material.
†Post failure.

In Figure 11, the kinetic energy of the pendulum mass dissipated by the post/soil system is shown in curves plotted against embedment depth for the two soil types and three post specimen widths. Values of the Soil Type 2 curves appear to vary exponentially with embedment while Soil Type 1 curves are practically linear. Furthermore, the Soil Type 2 curves become almost vertical at embedment depth of 40 inches.

The average post/soil system resistance force F* is shown in Figure 12 as a function of soil type and post embedment. These curves are similar in shape to the kinetic energy plots (Fig. 11) since they are obtained by dividing kinetic energy by a fairly consistent post deflection. Average force F increases directly with embedment and post width. Also, the average force varies directly with the standard penetrometer test (0.6 and 12 blows/ft for Soil Types 1 and 2, respectively) although additional soils would be required to define the relationship.

Comparison between static and dynamic force-deflection results are shown in Figure 13 for Soil Type 1 and in Figure 14 for Soil Type 2. Also, these results are compared in Table 4. Excluding the inertia peak in Figure 13, the dynamic resistance force has a

*See Appendix A for definition and determination.

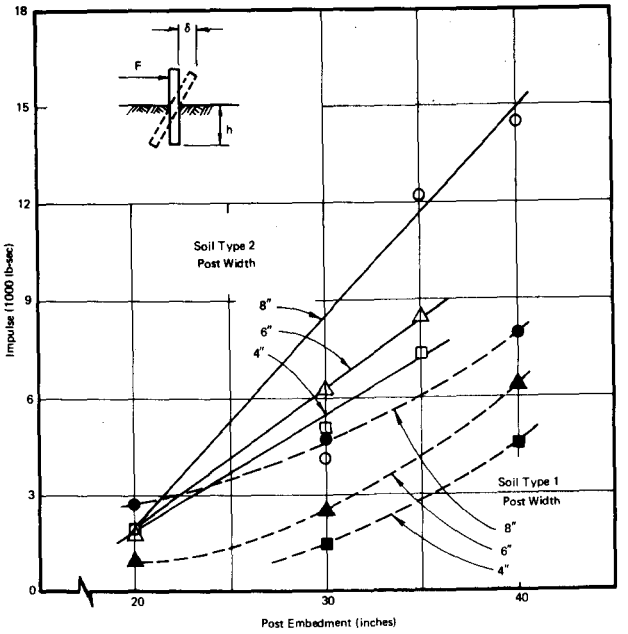

Figure 10. Relationship of post/soil system impulse with embedment.

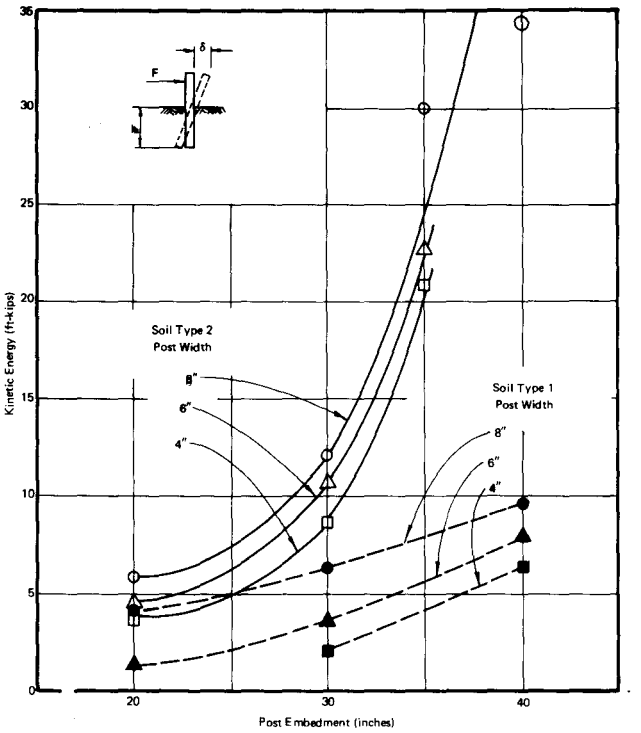

Figure 11. Relationship of post/soil system kinetic energy dissipation with post embedment.

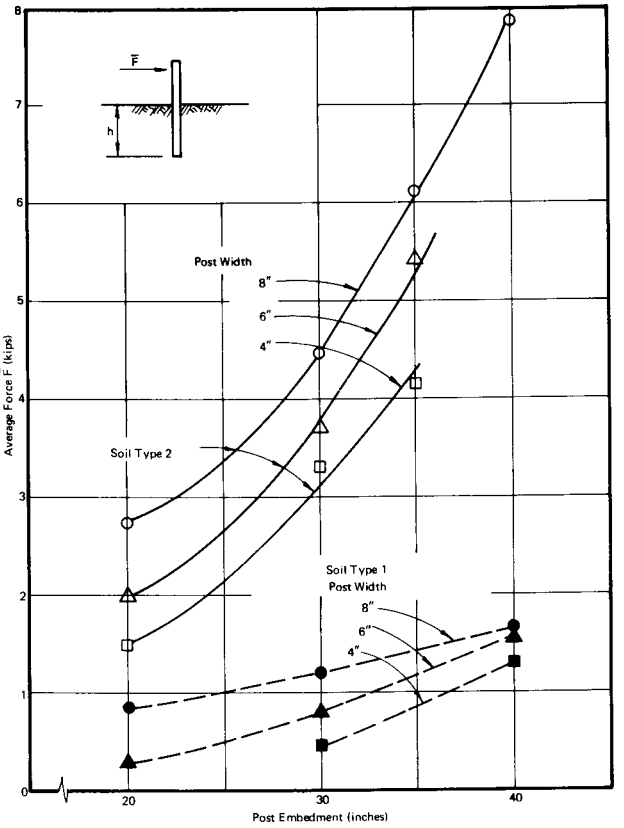

Figure 12. Relationship of post/soil average resistance force with post embedment.

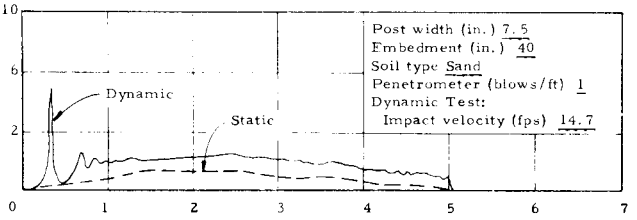

Figure 13. Comparison of static and dynamic force deflection curves for Soil Type 1.

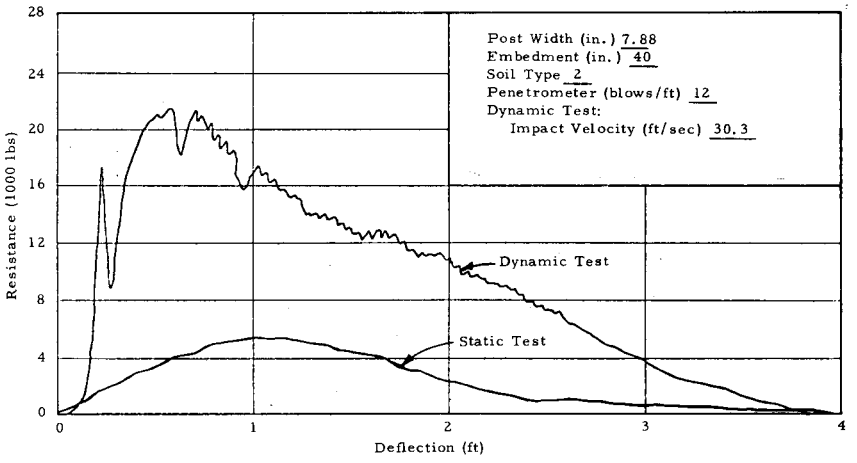

Figure 14. Comparison of static and dynamic force deflection curves for Soil Type 2.

Table 4. Comparison of dynamic and static post/soil test results.

Factors	Results* Static	Dynamic	Ratio
Type 1 Soil			
Maximum Force (kips)	1.4	2.0†	1.4
Average Force (kips)	0.7	1.6	2.2
Energy Dissipated (ft-kips)	3.7	8.4	2.3
Type 2 Soil			
Maximum Force (kips)	5.3	21.5	4.1
Average Force (kips)	2.0	8.7	4.0
Energy Dissipated (ft-kips)	8.0	33.4	4.2

*8 X 8-in. post embedded 40 inches.
†Excludes inertia peak.

maximum value of 2.0 kips; the statically applied load exhibits a maximum value of 1.4 kips. The ratio of energy dissipated by the post/Soil Type 1 system is 2.3 (Table 4). The contrast between dynamic and static properties is more pronounced for Soil Type 2. As shown in Figure 14, peak (or maximum) resistance forces are 21.5 kips dynamic and 5.3 kips static; energy dissipation values are 33.4 ft-kips dynamic and 8.0 ft-kips static; average resistance forces are 8.7 kips dynamic and 2.0 kips static. It is interesting to note that the ratios of dynamic to static post/Soil Type 2 properties are approximately four for peak force, average force, and energy dissipation parameters.

Typical post/soil failure characteristics are shown in Figure 15 for both dynamic and static tests.

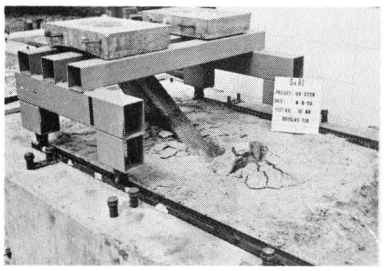

a. Type 1 Soil Static Test

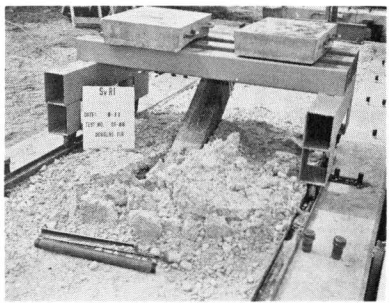

b. Type 2 Soil Static Test

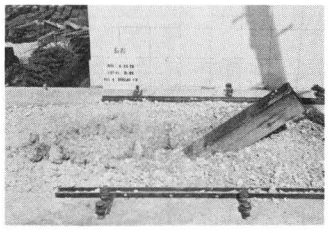

c. Type 2 Soil Dynamic Test

Figure 15. Typical post/soil failure characteristics.

IV. DISCUSSION

The project was designed as an exploratory program to identify the more significant post/soil parameters and the range of dynamic responses. Also, the experimental procedure and testing apparatus were investigated as to their utility, precision, and control. Accordingly, results presented herein should be viewed as tentative, awaiting verification by a more comprehensive program. However, the data, findings, and results are considered unique and meaningful and may have immediate use in upgrading existing traffic barrier systems. It should be emphasized that the test results are directly dependent on the test method employed; hence, any extrapolation of results to other conditions should be performed with care.

There are several observations concerning the experimental program and the program results; these observations are discussed in the following sections.

A. Experimental Procedure

1. Apparatus

The initial design of the pendulum mass bumper provided for a direct mass-to-post specimen contact. Also, a steel box beam section was used in the initial tests as the post specimen. However, the mass and stiffness of the steel member produced an excessive onset of acceleration in the pendulum mass and damaged the accelerometers. To attenuate the onset rate, an elastomer pad was attached to the specimen in the mass bumper contact area. Also, a timber post was employed in lieu of the box beam to reduce the specimen weight. No change was made to the repaired accelerometer, which was hard-mounted to the mass bumper.

It was also observed in the initial tests that the specimens' inertia response was a significant portion of the total impulse curve. To minimize the inertia effect (see Figs. 9 and 13), the impact velocity was reduced from 30 fps to 20 and 15 fps in a number of tests. However, for the 40-in. embedment tests, a 30-fps velocity was necessary to fail the specimen/soil system. The effect of varying impact velocity from 30 to 15 fps does not appear to influence results to a meaningful degree; this observation is based on the fact that the plots in Figures 10, 11, and 12 represent data from the range of test velocities, yet the curves are smooth and continuous. On the other hand, if very low impact velocities were used, for example, near 1 fps, it is surmised that results would approach those from the static test conditions.

2. Soils

The two soils investigated are classified as noncohesive and were selected to give a broad range of specimen support. Soil Type 1 provided a minimum specimen support as illustrated by the penetrometer test (0.6 blow per foot). Soil Type 2 is more typically found on highway shoulders where guardrail systems are installed.

A well-graded, intermediate aggregate with minimum fines (minus No. 100 mesh) was examined before Soil Type 2 was selected; however, a preliminary test indicated the results were similar to Soil Type 1. Although it was also recognized that the fines could

cause the soil to become sensitive to moisture content, it was concluded that some fines were necessary to produce desired soil strength.

3. Specimens

Principal concern of the program was to investigate the soil behavior, maintaining properties of the post constant. The initial program plan was to use a steel box section "strong post" specimen in order to eliminate the possibility of post failure from the results. However, as previously discussed, it was necessary to employ a less stiff timber specimen to prevent damage to the data acquisition instrumentation. As a result, post failures occurred in several tests of small posts/large embedment conditions; hence, 40-in. embedment, 4-in.-wide specimen tests in Soil Type 2 resulted in post fracture prior to extensive soil deformation.

By maintaining the length of post specimens extending above grade at a constant 32 in., the overall length of specimens varied from 52 to 72 in. for embedments of 20 and 40 in., respectively. The effect of this specimen length variation or mass variation is readily apparent from program results. However, it is surmised to be of secondary order of magnitude.

B. Post/Soil Parameters

As expected, the three post/soil system parameters of (1) soil strength, (2) specimen width, and (3) specimen embedment depth exhibit primary influence on the dynamic response of the specimens. Soil strength and embedment depth appear to be the more important parameters, while specimen width indicates a less important function.

Specimen thickness (i.e., dimension in plane of loading) was not investigated in this program. However, it is conjectured that thickness may be important where the specimen has a rough surface or the soil is cohesive.

V. CONCLUSIONS

From the program findings, several conclusions can be drawn. Due to the fact that the program is an exploratory investigation, these conclusions pertain to gross dynamic post/soil properties and are considered tentative, awaiting a more comprehensive examination.

A. Soil Effects

(1) Dynamic resistance force (peak and average) and kinetic energy absorbed by noncohesive soils are significantly related to the soil strength as determined by a standard penetrometer test.

(2) The soil strength effect becomes more pronounced for greater embedment depths (i.e., more than 30 in.).

(3) The ratio of dynamic-to-static soil properties increases with soil strength (i.e., from a range of 2 to 4).

B. Embedment Geometry

(1) Dynamic resistance force (peak and average) and kinetic energy absorbed by the soil are directly related to the *specimen width;* this conclusion was true for both soils and all embedment depths investigated.

(2) Dynamic resistance force (peak and average) and kinetic energy absorbed by the soil are significantly affected by and directly related to *specimen embedment depth.* Embedment depth has a more pronounced influence on post/soil system properties for the higher strength soil (i.e., Soil Type 2).

(3) The effect of post specimen thickness (i.e., dimension in plane of loading) is undetermined as this parameter was beyond the program scope.

C. Relationship of Static-to-Dynamic Results

(1) Peak and average resistance force and energy absorbed by the post/soil system are greater for the dynamically applied post displacement. The ratio of dynamic-to-static properties is greater (i.e., 4 versus 2) for the higher strength soil (i.e., Soil Type 2).

(2) The post/soil systems offered resistance through an approximate 4-ft displacement for static and dynamic tests.

(3) No definite relationship can be established between dynamic-to-static post/soil properties based on the results of this program.

APPENDIX A
SAMPLE CALCULATIONS

SAMPLE CALCULATIONS

The following calculations are employed in scaling, converting, and processing experimental data from the pendulum impact facility. The basic data consist of a continuous recording of accelerometer output during specimen impact.

1. Determine acceleration magnitude of pendulum mass at time t

$$A_t = \left(\frac{d_t}{d_c}\right) A_c \tag{1}$$

where d_c is Visicorder trace deflection (in.) due to reference calibration signal corresponding to A_c acceleration (g's), and d_t is Visicorder trace deflection (in.) at any time t during test.

Example: For case where d_c, A_c, and d_t are 2.98 in., 5.2 g's and 0.75 in., respectively, then

$$A_t = \left(\frac{0.75}{2.98}\right)(5.2) = \underline{1.31 \text{ g's}}$$

2. Determine magnitude of force acting on pendulum mass at time t. (Note, this is equal to but in opposite direction to the force acting on the post.)

$$F_t = ma_t \tag{2}$$

where m is pendulum mass (lb-sec^2)/ft and a_t (ft/sec^2) is acceleration (or deceleration) of mass.

Example: For case where pendulum weighs 4000 lb and a_t is 1.31 g's

$$F_t = \left(\frac{4000}{g}\right)(1.31 \text{ g}) = \underline{5240 \text{ lb}}$$

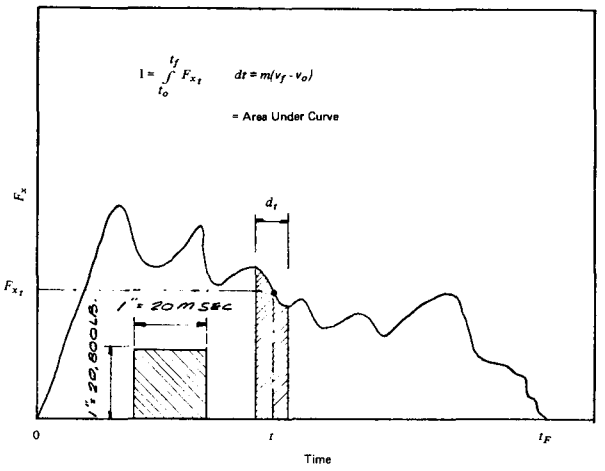

Figure A.1. Pendulum mass linear impulse determination.

3. Determine velocity of pendulum mass after impact. By Newton's second law of motion, the linear impulse is equal to the change in linear momentum of the pendulum mass

$$\int_{t_o}^{t_f} F_{x_t}\, dt = m(v_f - v_o) \tag{3}$$

where F_{x_t} is the resultant force acting on the pendulum mass in the x direction at time t, m is the pendulum mass, and v_o and v_f are the initial and final velocities of the mass in the x direction. A typical force-time curve is shown in Figure A.1; by definition linear impulse is equal to the area under the curve.

Example: The time scale in Figure A.1 is 20 ms/in. and the force scale is 20,800 lb/in.; thus 1.0 sq in. of area represents linear impulse of (0.020) (20,800) or 416 lb-sec/in.^{2}. The area under the curve is determined to be 6.50 sq in., initial velocity of the mass is 30.3 fps and the mass weighs 4000 lb; then the final velocity can be calculated:

$$\int_{t_o}^{t_f} F_{x_t}\, dt = (\text{Area})(K) = m(v_f - v_o)$$

$$-(6.50)(416) = \frac{4000}{32.2}\ (v_f - 30.3) \tag{3}$$

$$v_f = (30.3 - 21.8) = \underline{8.5 \text{ fps}}$$

4. Determine the energy dissipated in fracturing the post specimen. The work ΔU done by force F_x on the pendulum mass during movement d_x is equal to the change in kinetic energy ΔT of the mass; this is also the fracture energy of the post specimen.

$$\Delta U = \Delta T$$

$$\int_{o}^{x} F_x\, dx = \frac{1}{2} m(v_f^2 - v_o^2) \tag{4}$$

Example: Initial and final velocities are 30.3 and 8.5 fps, respectively. Then the change in kinetic energy (fracture energy) is

$$\Delta T = \frac{1}{2} m(v_f^2 - v_o^2) = \frac{4000}{2(32.2)}(8.5)^2 - (30.3)^2 = \underline{52{,}500 \text{ ft-lb}}$$

5. Calculate post displacement during impact. Assume mass velocity changes linearly with time; thus

$$d' = \left(\frac{v_f + v_o}{2}\right)(t_f - t_o) \tag{5}$$

where v_f, v_o, t_f, and t_o are respectively final and initial velocities and final and initial time.

Example: Let v_f and v_o be 30.3 and 8.5 fps and t_f and t_o be 200 and 0 ms; then

$$d = \left(\frac{8.5 + 30.3}{2}\right)(200 - 0) = \underline{3.88 \text{ ft}}$$

6. Calculate the average force during specimen displacement

$$\int_{o}^{x} F_x\, dx = \bar{F}_x d' = \Delta U \tag{4}$$

where $\overline{F}_x$ is an idealized constant force that acts through distance d' (see Figure A.2).

Example: Let ΔU be 52,500 ft-lb and d' be 3.88 ft; then

$$\overline{F}_x = \left(\frac{U}{d'}\right) = \left(\frac{52{,}500}{3.88}\right) = \underline{13{,}520 \text{ lb}}$$

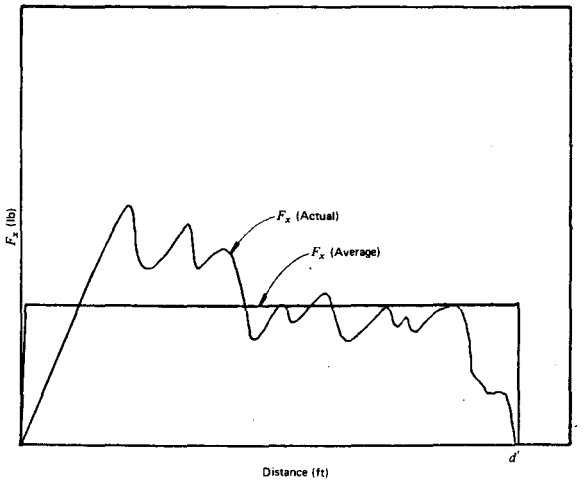

Figure A.2. Relationship between actual and average force.

APPENDIX B

SAMPLE IMPULSE PLOTS

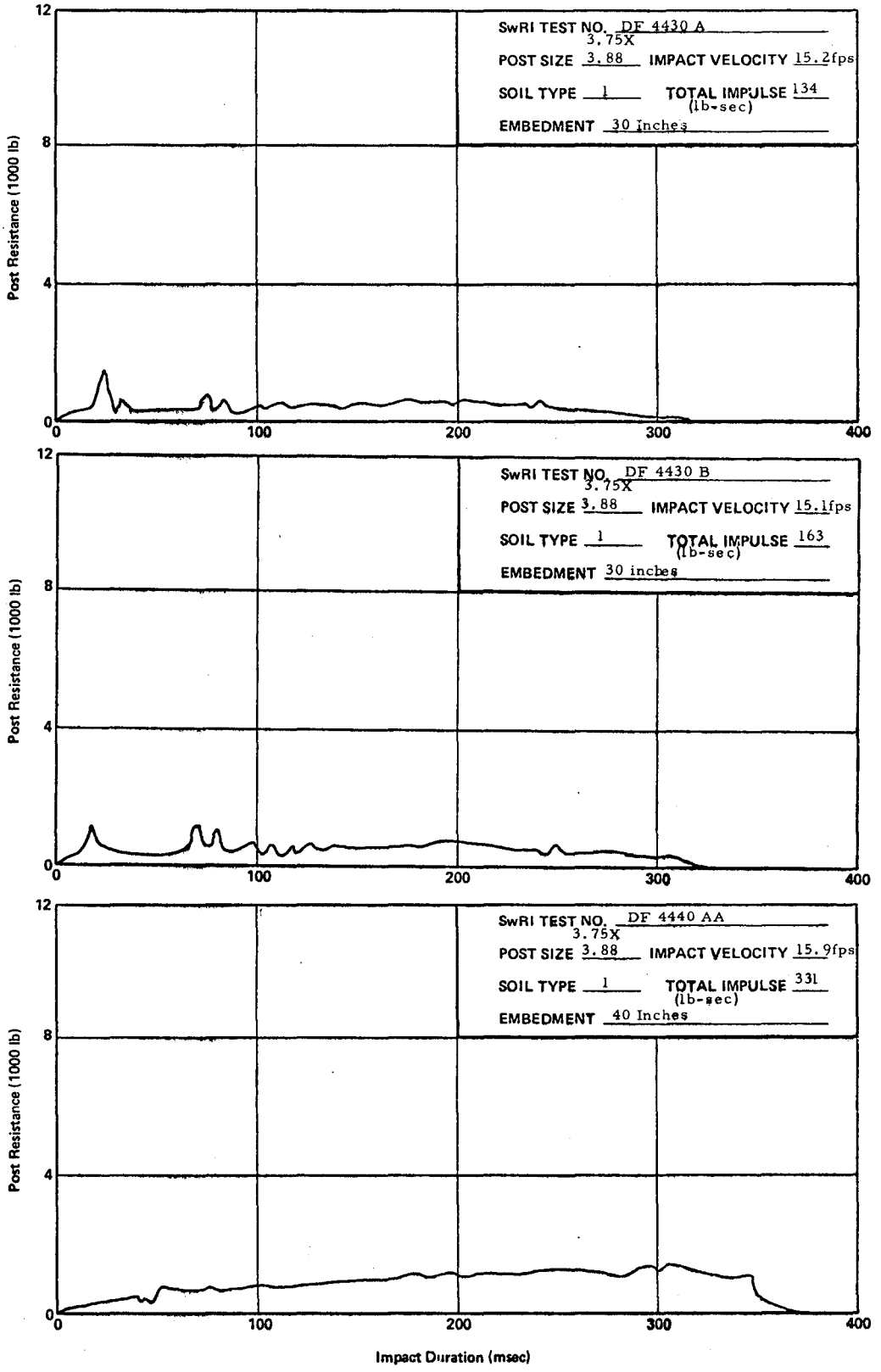

Figure B.1. Sample impulse plots for Soil Type 1.

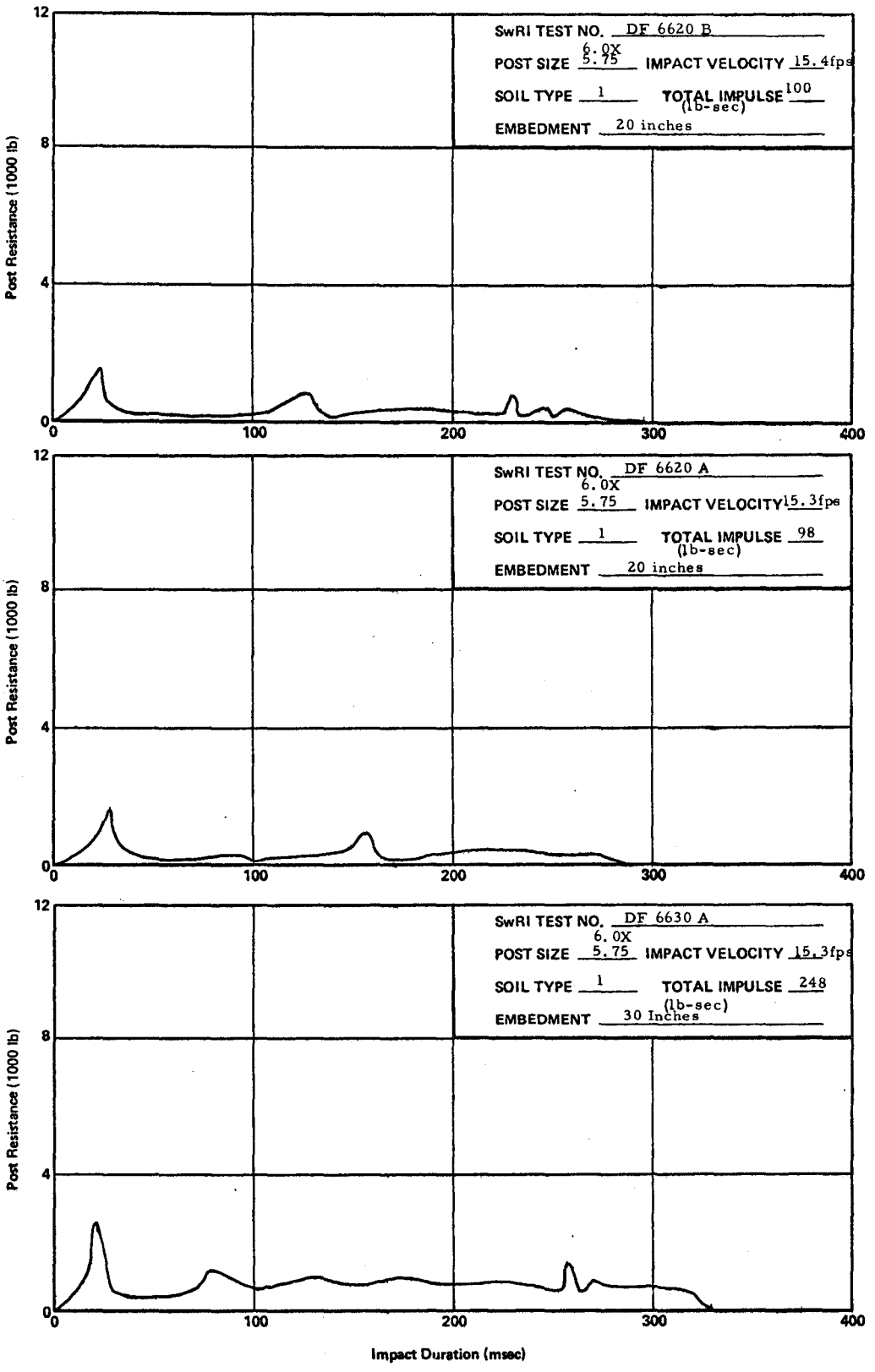

Figure B.1. Sample impulse plots for Soil Type 1 (cont'd).

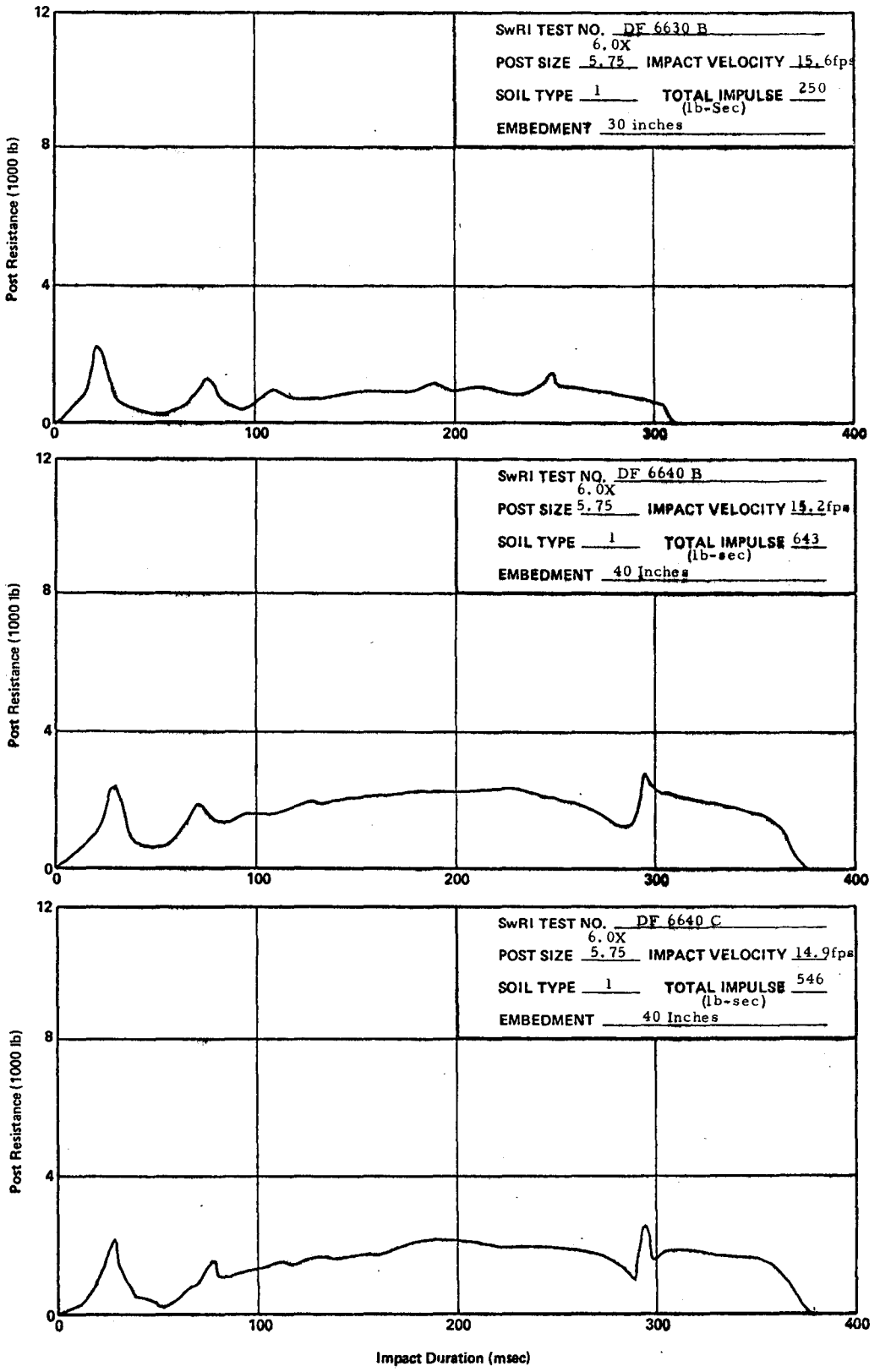

Figure B.1. Sample impulse plots for Soil Type 1 (cont'd).

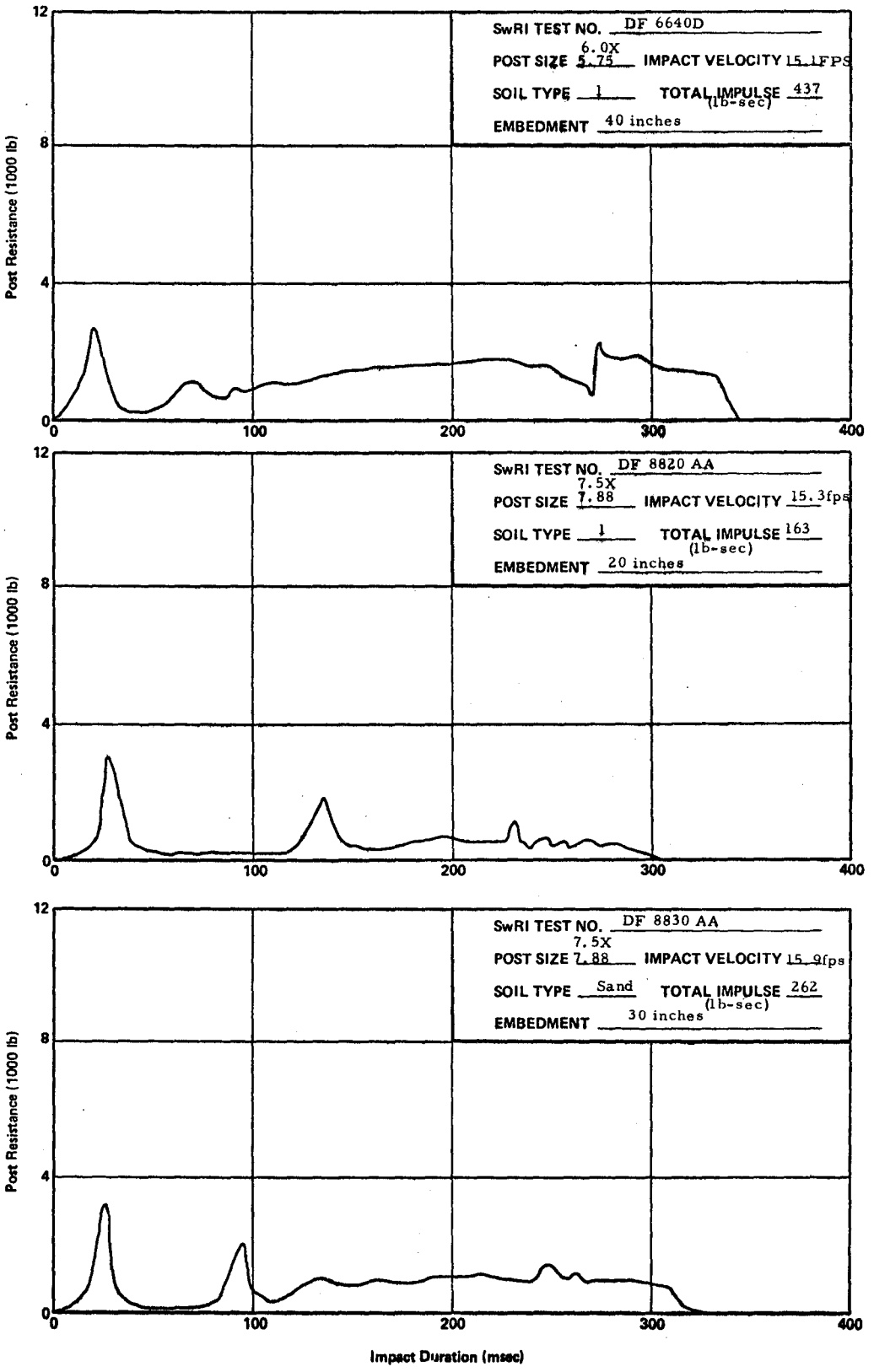

Figure B.1. Sample impulse plots for Soil Type 1 (cont'd).

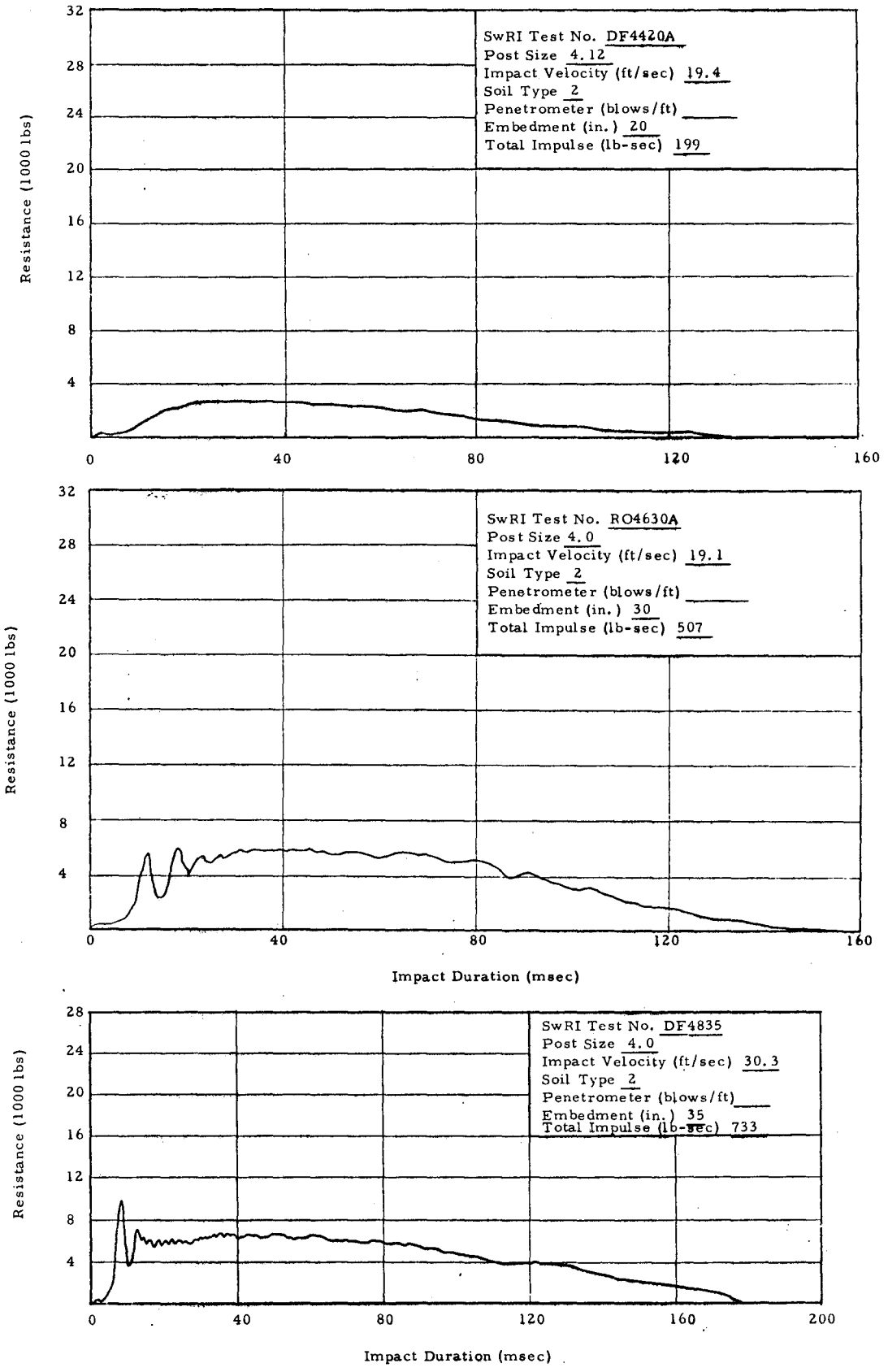

Figure B 2 Sample impulse plots for Soil Type 2

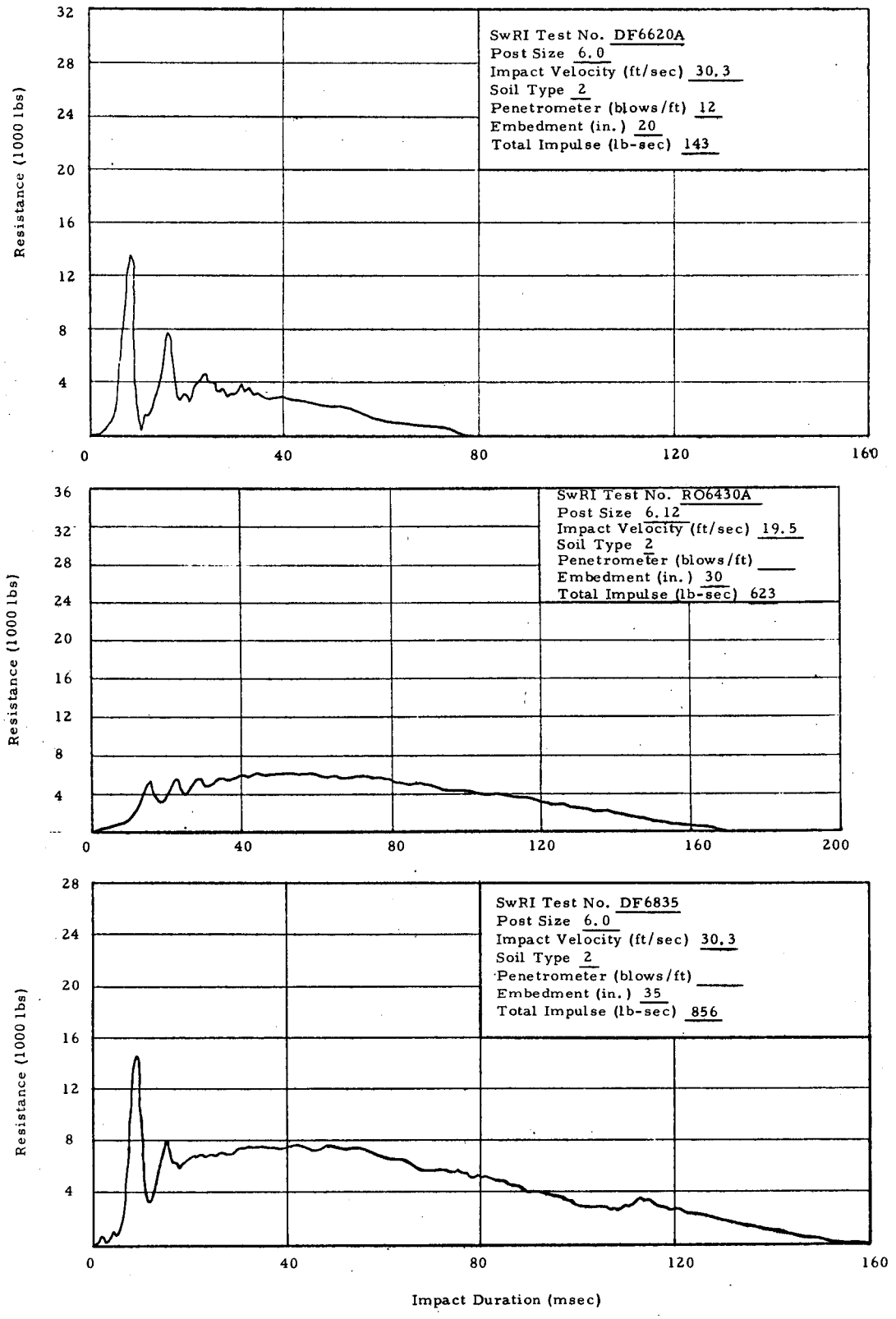

Figure B.2. Sample impulse plots for Soil Type 2 (cont'd).

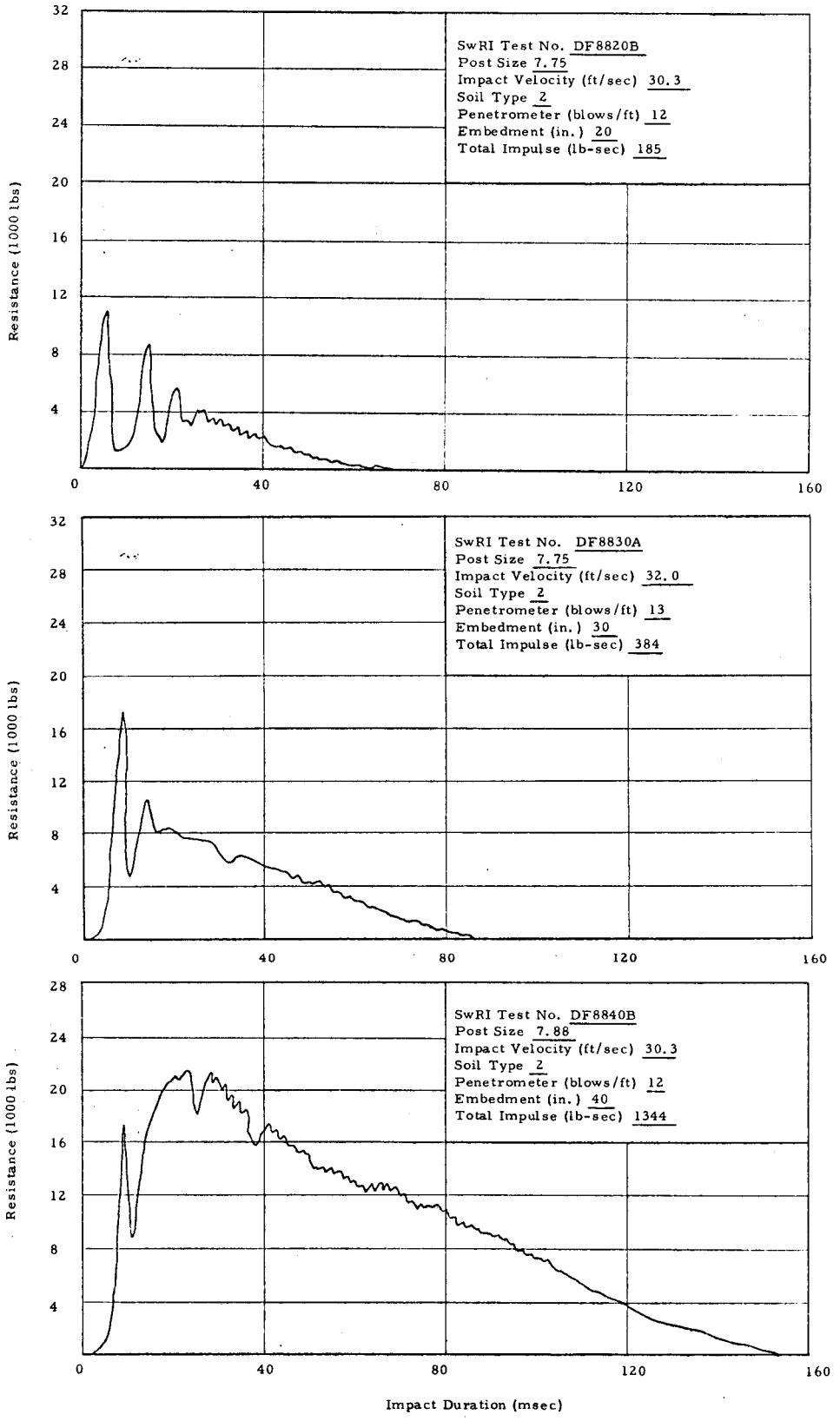

Figure B.2. Sample impulse plots for Soil Type 2 (cont'd).